

Modeling Arsenic(III) Adsorption and Heterogeneous Oxidation Kinetics in Soils

Bruce A. Manning* and Donald L. Suarez

ABSTRACT

Arsenite [As(III)] is a soluble and toxic species of arsenic that can be introduced into soil by geothermal waters, mining activities, irrigation practices, and disposal of industrial wastes. We determined the rates of As(III) adsorption, and subsequent oxidation to arsenate [As(V)] in aerobic soil–water suspensions using four California soils. The rate of As(III) adsorption on the soils was closely dependent on soil properties that reflect the reactivity of mineral surfaces including citrate–dithionite (CD) extractable metals, soil texture, specific surface area, and pH. Heterogeneous oxidation of As(III) to As(V) was observed in all soils studied. The recovery of As(V) from As(III)-treated soils was dependent on levels of oxalate-extractable Mn and soil texture. After derivation of rate equations to describe the changes in soluble and recoverable As(III) and As(V) in soil suspensions, soil property measurements were used to normalize the empirically derived rate constants for three soils. The fourth soil, which had substantially different soil properties from the other three soils, was used to independently test the derived soil property–normalized model. The soil property–normalized consecutive reaction model gave a satisfactory description of the trends seen in the experimental data for all four soils. Understanding the effects of soil properties on the kinetics of chemical reactions of As(III) and As(V) in soils will be essential to development of quantitative models for predicting the mobility of As in the field.

THE OXIDATION of trace metals and metalloid oxyanions by soils has an important role in determining their mobility and toxicity. Reduced species such as As(III), Se(IV), and Cr(III) can be oxidized in soils to produce As(V), Se(VI), and Cr(VI), respectively. In the case of Se and Cr, the oxidized Se(VI) and Cr(VI) species are less strongly adsorbed to soils than Se(IV) and Cr(III) and thus are more mobile and bioavailable. The oxidation of As(III) produces As(V), which is strongly adsorbed in soils and is less toxic than As(III) (Knowles and Benson, 1983). Despite the fact that the reactions of As(III) with soil have been studied, the rates and mechanisms of As(III) adsorption, as well as oxidation to As(V), are still not well understood. The As(III) species can also be present in groundwater (Korte and

Fernando, 1991), and therefore the stability of As(III) after coming in contact with aerobic soils is of interest in environmental management.

Previous work on the reactions of As(III) with soil has focused primarily on As(III) adsorption rather than As(III) oxidation (Manning and Goldberg, 1997a; McGeehan and Naylor, 1994; Elkhatib et al., 1984). Iron oxides have been shown to be the most important mineral component in determining a soil's overall capacity to adsorb As(III) and As(V) (Jacobs et al., 1970; Fordham and Norrish, 1974, 1979; Elkhatib et al., 1984; Livesey and Huang, 1981; Manning and Goldberg, 1997a). It has also been concluded, using x-ray absorption spectroscopy (XAS), that As(V) is specifically adsorbed on synthetic Fe(III) oxide mineral surfaces (Waychunas et al., 1993; Fendorf et al., 1997). Electrophoretic mobility work (Pierce and Moore, 1982) has shown that As(III) is also specifically adsorbed on the Fe(III) oxide surface, and this has now been confirmed using Fourier transform infrared spectroscopy (Sun and Doner, 1996) and XAS (Manning et al., 1998).

The oxidation of As(III) to As(V) in soils has not been extensively studied despite the fact that this is an important reaction in the cycling of As in the environment. The oxidation of As(III) by lake sediments has been investigated (Oscarson et al., 1980, 1981) and it was concluded that an abiotic process involving Mn oxide minerals was directly responsible for As(III) oxidation. Heterogeneous oxidation of As(III) by synthetic Mn oxides (Oscarson et al., 1983; Scott and Morgan, 1995; Sun and Doner, 1998), and clay minerals (Manning and Goldberg, 1997b) has been shown, though very little is known about the rates or mechanisms of As(III) oxidation in whole soils. An improved understanding of the rate of As(III) oxidation in whole soil is necessary for the application of predictive models to describe As transport in the field. In addition, linking measurements of important soil properties with a quantitative description of As(III) adsorption and oxidation would improve the predictive capability of reactive transport models.

Given the need for a better understanding of the

Bruce A. Manning, Dep. of Chem. and Biochem., San Francisco State Univ., 1600 Holloway Ave., San Francisco, CA 94132; and Donald L. Suarez, USDA-ARS, U.S. Salinity Lab., 450 W. Big Springs Rd., Riverside, CA 92507-4617. Contribution from the USDA-ARS U.S. Salinity Lab. Received 19 Aug. 1998. *Corresponding author (bmanning@sfsu.edu).

Published in Soil Sci. Soc. Am. J. 64:128–137 (2000).

Abbreviations: CD, citrate–dithionite; DI, deionized; HPLC–HGAAS, high performance liquid chromatography–hydride generation atomic absorption spectrometry; Me_F, total citrate–dithionite extractable metals (Al + Fe + Mn); Mn_{OX}, oxalate-extractable manganese; SA, specific surface area; XAS, x-ray absorption spectroscopy; XRD, x-ray diffraction.

oxidation and adsorption rates of As(III) in soils, the objectives of this study were: (i) to determine the As(III) adsorption and oxidation rates in soil by measuring the As(III)–As(V) speciation and fractionation in As(III)-treated soil as a function of time; (ii) to develop a simple, verifiable kinetic rate law for describing the time-dependent reactions of As(III) in soil for eventual use in solute transport models; and (iii) to incorporate soil property measurements into kinetic expressions to improve their general applicability to different soils.

THEORY

Two techniques can be used to describe time-dependent reactions in well-mixed soil suspensions: (i) mechanistic rate law determination and (ii) apparent rate law determination (Sparks, 1989, p. 5–11; Skopp, 1986). Mechanistic rate law determination describes elementary chemical reactions at the molecular level, whereas an apparent rate law recognizes that unknown elementary reactions may be contributing to an overall, apparent rate. Even in well-mixed, dilute soil suspensions, modeling the rate of As(III) adsorption and oxidation is complicated by intraparticle diffusion, unknown reaction intermediates, and irreversible adsorption of both reactants and products. Therefore, modeling As(III) adsorption and oxidation in soil suspensions is best treated by defining apparent rate laws for the measurable processes after treatment of the soil with As(III).

We used the following mass balance expression for the measurable fractionation of As(III) in soil suspensions:

$$[\text{As(III)}]_0 = [\text{As(III)}]_{\text{sol}} + [\text{As(V)}]_{\text{sol}} + [\text{As(III)}]_{\text{exch}} + [\text{As(V)}]_{\text{exch}} + [\text{As}]_{\text{immobile}} \quad [1]$$

where $[\text{As(III)}]_0$ is initial As(III) added to the suspension; $[\text{As(III)}]_{\text{sol}}$ and $[\text{As(V)}]_{\text{sol}}$ are soluble As(III) and As(V); $[\text{As(III)}]_{\text{exch}}$ and $[\text{As(V)}]_{\text{exch}}$ are exchangeable As(III) and As(V); and $[\text{As}]_{\text{immobile}}$ is immobile, or unrecoverable, As. The $[\text{As(III)}]_{\text{exch}}$ and $[\text{As(V)}]_{\text{exch}}$ fractions were operationally defined by recovery using a phosphate extraction procedure (see below). The $[\text{As}]_{\text{immobile}}$ fraction was operationally defined as all “unrecoverable” As, or the difference between $[\text{As(III)}]_0$ and total recoverable As, which can be expressed by rearrangement of Eq. [1]:

$$[\text{As}]_{\text{immobile}} = [\text{As(III)}]_0 - [\text{As(III)}]_{\text{sol}} - [\text{As(V)}]_{\text{sol}} - [\text{As(III)}]_{\text{exch}} - [\text{As(V)}]_{\text{exch}} \quad [2]$$

Using the mass balance expressions in Eq. [1] and [2], two apparent rate laws were developed to describe the fractionation of As(III) after addition to the soil: Case 1, rates of change in soluble As(III) and As(V), and Case 2, rates of change in recoverable As(III) and As(V).

Case 1: Soluble As(III) and As(V)

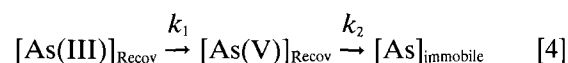
The rates of change in soluble As(III) and As(V) were described with the following expression:

$$[\text{As(III)}]_{\text{sol}} \xrightarrow{k_1} [\text{As(V)}]_{\text{sol}} \rightarrow [\text{As}]_{\text{immobile}} \quad [3]$$

where k_1 and k_2 are the forward rate constants (h^{-1}) for the reactions. Equation [3] is an apparent rate expression because it does not describe elementary chemical reactions and only accounts for the measurable changes in the soluble As(III) and As(V) species. Modeling the transport of As(III) and As(V) in the field will require a kinetic expression to describe the time-dependent changes in $[\text{As(III)}]_{\text{sol}}$ and $[\text{As(V)}]_{\text{sol}}$. In addition, the inclusion of $[\text{As}]_{\text{immobile}}$ in Eq. [3] is important because this is a long-term sink for As in soil.

Case 2: Total Recoverable As(III) and As(V)

A second rate expression was used to describe the rate of change in the amounts of total recoverable As(III) and As(V) in soil suspensions treated with As(III):



where $[\text{As(III)}]_{\text{Recov}}$ and $[\text{As(V)}]_{\text{Recov}}$ are total recoverable (soluble + exchangeable) As(III) and As(V), respectively. Case 2 is an attempt to describe the total As(III) and As(V) in the suspension (soil + solution) and conforms to the mass balance of the system in Eq. [1] where:

$$[\text{As(III)}]_0 = [\text{As(III)}]_{\text{Recov}} + [\text{As(V)}]_{\text{Recov}} + [\text{As}]_{\text{immobile}} \quad [5a]$$

where:

$$[\text{As(III)}]_{\text{Recov}} = [\text{As(III)}]_{\text{sol}} + [\text{As(III)}]_{\text{exch}} \quad [5b]$$

and

$$[\text{As(V)}]_{\text{Recov}} = [\text{As(V)}]_{\text{sol}} + [\text{As(V)}]_{\text{exch}} \quad [5c]$$

Equation [4] closely describes the rate of change in total As(III) in the soil suspension system ($[\text{As(III)}]_{\text{sol}} + [\text{As(III)}]_{\text{exch}}$).

Consecutive Reaction Mechanisms

The mathematical treatment of Eq. [3] and [4] uses the theory of consecutive reaction mechanisms (Laidler and Meiser, 1982, p. 406–409). Using Eq. [4] as an illustration, the first-order kinetic expression for the rate of decrease in $[\text{As(III)}]_{\text{Recov}}$ is:

$$\frac{d[\text{As(III)}]_{\text{Recov}}}{dt} = -k_1[\text{As(III)}]_{\text{Recov}} \quad [6]$$

Equation [6] was then integrated using the boundary condition $[\text{As(III)}]_{\text{Recov}} = [\text{As(III)}]_0$ when $t = 0$, which gives:

$$[\text{As(III)}]_{\text{Recov}} = [\text{As(III)}]_0 \exp(-k_1 t) \quad [7]$$

A natural log transformation of experimental data ($\ln[\text{As(III)}]/[\text{As(III)}]_0$) was made and plotted vs. t (h) and the following linearized version of Eq. [7] was fit to the $[\text{As(III)}]_{\text{Recov}}$ data:

$$\ln\left(\frac{[\text{As(III)}]_{\text{Recov}}}{[\text{As(III)}]_0}\right) = -k_1 t \quad [8]$$

The value of k_1 was derived from linear regression analy-

sis. The rate of change in $[\text{As(V)}]_{\text{Recov}}$ is described by:

$$\frac{d[\text{As(V)}]_{\text{Recov}}}{dt} = k_1[\text{As(III)}]_{\text{Recov}} - k_2[\text{As(V)}]_{\text{Recov}} \quad [9]$$

Substituting Eq. [7] into [9] gives:

$$\frac{d[\text{As(V)}]_{\text{Recov}}}{dt} = k_1[\text{As(III)}]_0 \exp(-k_1 t) - k_2 [\text{As(V)}]_{\text{Recov}} \quad [10]$$

Integrating and rearranging Eq. [10] gives the following expression:

$$[\text{As(V)}]_{\text{Recov}} = [\text{As(III)}]_0 \left(\frac{k_1}{k_2 - k_1} \right) [\exp(-k_1 t) - \exp(-k_2 t)] \quad [11]$$

Equation [11] was fitted to experimental $[\text{As(V)}]_{\text{Recov}}$ data using k_1 from Eq. [8] and optimizing k_2 through minimization of the sums of squares of differences between the experimental and model values ($\sum\{[\text{As(V)}]_{\text{Recov}} - [\text{As(V)}]_{\text{Model}}\}^2$) (Steel and Torrie, 1980). To predict the formation of $[\text{As}]_{\text{immobile}}$ in soil suspensions as the final reaction product of As(III) with soil, Eq. [5a] was rearranged as:

$$[\text{As}]_{\text{immobile}} = [\text{As(III)}]_0 - [\text{As(III)}]_{\text{Recov}} - [\text{As(V)}]_{\text{Recov}} \quad [12]$$

Equations [7] and [11] were then combined with Eq. [12] to give:

$$[\text{As}]_{\text{immobile}} = \frac{[\text{As(III)}]_0}{(k_2 - k_1)} \{k_2[1 - \exp(-k_1 t)] - k_1[1 - \exp(-k_2 t)]\} \quad [13]$$

This expression was used to predict $[\text{As}]_{\text{immobile}}$ using $[\text{As(III)}]_0$, k_1 , and k_2 .

Incorporating Soil Property Data into Rate Equations

When applied to different soil types, the predictive capability of rate models will improve if important soil properties are used in the development of model equations. In our study, soil properties that influence the reactions of As(III) with soil such as CD-extractable Al + Fe + Mn (Me_T), oxalate-extractable Mn (Mn_{OX}), pH, and soil texture were used to normalize soil-specific rate constants. This allowed the derivation of normalized rate constants to be used in combination with measured soil-specific properties in rate expressions. Rate constants (k_{1i} and k_{2i}) for three soils (Fallbrook, Panoche, and Indio) were first fit directly to experimental data in the consecutive reaction model as described above. This was followed by correcting the fitted, empirical k_{1i} and k_{2i} values for three soils ($n = 3$) with soil property values:

$$k_1^N = \frac{\sum_i^n (k_{1i} (X_i Y_i)^{-1})}{n} \quad [14]$$

where k_1^N is the soil property-normalized rate constant

for the first step of the consecutive reaction model, k_{1i} is the empirically fitted k_1 for soil i , and X_i and Y_i are soil properties values for soil i . For the final modeling step, a new rate constant was recalculated for each soil:

$$k_1^{\text{soili}} = k_1^N X_i Y_i \quad [15]$$

where k_1^{soili} is the final calculated k_1 for soil i . Incorporating Eq. [15] into Eq. [7], for example, gives:

$$\begin{aligned} [\text{As(III)}]_{\text{Recov}}^{\text{soili}} &= [\text{As(III)}]_0 \exp(-k_1^{\text{soili}} t) \\ &= [\text{As(III)}]_0 \exp(-k_1^N X_i Y_i t) \end{aligned} \quad [16]$$

At most, two soil properties were used for rate constant normalization and incorporation into the consecutive reaction rate model. The influence of soil properties on the adsorption and oxidation of As(III) will be addressed in more detail below.

MATERIALS AND METHODS

Soil Characterization

Four soils from California were used in this study to represent a range of soil properties. Surface (<20 cm) samples of a Fallbrook sandy loam (fine-loamy, mixed, thermic, Typic Haploxeralf), Indio very fine sandy loam (coarse-silty, mixed, calcareous, hyperthermic Typic Torrifluvents), Panoche clay loam (fine-loamy, mixed, superactive, thermic Typic Haplocambid), and Aiken clay soil (fine, parasesquic, mesic Xeric Haplohumult) were sieved (<2 mm) and handled so as to maintain field soil moisture conditions by refrigeration at 4°C in sealed high-density polyethylene tubs. Though natural As(III)-As(V) speciation may change during storage, the As(III) oxidizing capacity of the soils did not change when the soils were stored this way for several months. The Aiken soil was used as an independent test soil for the kinetics model after model optimization using the Fallbrook, Indio, and Panoche soils. The pH of the soil-As(III) solution suspensions was determined with a Corning semi-micro glass combination pH electrode and a Corning Ion Analyzer 150 (Corning Glass Works, Corning, NY).¹ Soil texture was determined by the hydrometer method (Gee and Bauder, 1986). Specific surface area (SA) of the <2-mm soil fraction was determined by single-point Brunauer-Emmett-Teller N_2 adsorption with a Quantisorb Jr. surface area analyzer (Quantachrome Corp., Syosset, NY). The dominant mineralogy of the soils was analyzed by separating the sand and clay fractions by sedimentation in deionized (DI) water and recovery of the suspended clay particles by centrifugation. The sand fraction was then repeatedly rinsed with DI water and both oriented slide and random powder mounts were analyzed by x-ray diffraction (XRD) for major mineral components.

Selective dissolution analyses were performed to determine the Al, Fe, and Mn content and crystallinity of the soils. A CD extraction was employed to extract total crystalline or free Fe oxides by shaking 4 g of soil in 120 mL of 0.57 M sodium citrate ($\text{Na}_3\text{C}_6\text{H}_5\text{O}_7 \cdot 5\text{H}_2\text{O}$) and 0.1 M sodium dithionite ($\text{Na}_2\text{S}_2\text{O}_4$) for 16 h (Holmgren, 1967). Dissolution of Fe oxides by CD extraction also releases coprecipitated Al and Mn. Amorphous or poorly crystalline Al, Fe, and Mn oxides were determined by extracting 4 g of soil in 120 mL of acidified ammonium oxalate buffer [0.175 M $(\text{NH}_4)_2\text{C}_2\text{O}_4$ + 0.1 M $\text{H}_2\text{C}_2\text{O}_4$, pH 3.0] for 2 h (Loeppert and Inskeep, 1996). For both extraction procedures, the suspensions were shaken, cen-

¹ Trade names are used only for the benefit of the reader and do not imply endorsement by the USDA.

trifuged (4100 g, 10 min) and 15-mL aliquots were removed, filtered (0.1 μm), and acidified with high purity HNO_3 . Samples were then analyzed for Al, As, Fe, and Mn by inductively coupled plasma atomic emission spectrometry. A low background level of As was detected in the CD extracts of the soils (<10 mg kg^{-1} As), which was substantially below the amount of As(III) added during adsorption experiments.

As(III) Reaction Kinetics

The reaction kinetics of As(III) with the soils were investigated in batch experiments using 40-mL polycarbonate centrifuge tubes. Two grams of soil were reacted with 20 mL of 66.7 μM As(III) in 5 mM CaCl_2 on a reciprocating shaker for 0.25, 0.5, 1, 1.5, 2, 3, 4, 8, 18, 24, and 48 h. All sample treatments were processed in duplicate and the averages of duplicates are reported in all figures. The As(III) adsorption and oxidation reactions were terminated by centrifuging (14 500 g, 5 min), decanting the supernatant, and filtering (0.1 μm). This process took ≈ 10 min, and it was confirmed that oxidation of soluble As(III) ceased after separation of the solution from the soil solids. The solids remaining in the reaction tubes were then resuspended and shaken for 1 h in 20 mL of 10 mM $\text{KH}_2\text{PO}_4\text{:K}_2\text{HPO}_4$ buffer at pH 7 (10 mM PO_4) to recover exchangeable As(III) and As(V) from the soil. This extraction procedure has been used in previous work with As(III)-treated clay minerals (Manning and Goldberg, 1997b), and the As(III)-As(V) speciation in the filtered, refrigerated extract was preserved for several days. Addition of 10 mM PO_4 to the As(III)-treated soil did not cause additional As(III) oxidation, but actually may have slowed the oxidation by adsorbing on available oxidative surfaces.

The Fallbrook soil, which gave the greatest recoverable As(V), was chosen for more detailed work to investigate the effects of pH on As(III) adsorption and oxidation. These experiments used the same reaction conditions as given above except that the soils were first equilibrated for 24 h in 5 mM CaCl_2 containing an appropriate quantity of HCl or NaOH to make the soil suspension pH of 5.0, 6.0, 7.0, and 8.0. The pH-adjusted Fallbrook suspensions were treated with As(III) by adding 0.1 mL of 13.3 mM As(III) to commence the timed experiment.

Speciation of As(III) and As(V) in all soil solutions and extracts was determined by high performance liquid chromatography (HPLC) using a Dionex AS-11 IonPac anion exchange column (Dionex Corp., Sunnyvale, CA) coupled with hydride generation atomic absorption spectrometry (HGAAS) detection (Manning and Martens, 1997). This technique allowed direct, trace-level detection of As(III) and As(V) in complex soil solution matrices. The majority of samples were analyzed by HPLC-HGAAS immediately after filtering, without sample storage.

RESULTS AND DISCUSSION

Soil Characteristics

Selected soil properties for the four soils are shown in Table 1. The soil pH values (1:10 soil/DI water) show a range from 9.3 for the Indio soil to 5.9 for the Aiken soil, indicative of the wide range in properties of these soils. The Indio and Fallbrook soils had similar particle-size distribution, dominated by sand, whereas the Panoche and Aiken soils were higher in clay-size particles. Specific surface area, clay content, and amount of extractable metals were closely related soil properties in these samples. Both the Fallbrook and Indio soil clay

Table 1. Selected properties of three California soils.

Property	Soil			
	Indio	Fallbrook	Panoche	Aiken
pH [†]	9.3	6.5	7.9	5.9
Sand, %	65	66	44	25
Silt, %	25	20	28	28
Clay, %	10	14	28	47
BET surface area, $\text{m}^2 \text{g}^{-1}$	7.12	19.4	27.6	44.8
$\text{Al}_{\text{OX}}, \text{mmol kg}^{-1}$	15.9	14.9	23.6	101
$\text{Fe}_{\text{OX}}, \text{mmol kg}^{-1}$	11.4	10.1	11.2	16.1
$\text{Mn}_{\text{OX}}, \text{mmol kg}^{-1}$	0.75	4.28	3.66	38.7
$\text{Al}_{\text{CD}}, \text{mmol kg}^{-1}$	20.0	24.7	36.7	161
$\text{Fe}_{\text{CD}}, \text{mmol kg}^{-1}$	43.1	115	157	229
$\text{Mn}_{\text{CD}}, \text{mmol kg}^{-1}$	1.02	3.60	3.59	38.6
$\text{Me}_e, \text{mmol kg}^{-1}$	64.1	143	197	429

[†] Measurement made after 48 h in 1:10 soil/As(III) solution suspensions.

[‡] BET = Brunauer-Emmett-Teller.

[§] OX = ammonium oxalate extract.

[¶] CD = citrate-dithionite extract.

[#] Me_e = total citrate-dithionite extractable metals ($\text{Al}_{\text{CD}} + \text{Fe}_{\text{CD}} + \text{Mn}_{\text{CD}}$).

fractions were composed of predominantly mica and illite with moderate amounts of kaolinite. However, the Indio soil, with both alkaline and sodic properties, also contained quartz and some calcite in the clay fraction. The clay fraction of Panoche clay loam was composed predominantly of illite. The XRD patterns of sand fractions were dominated by quartz and other primary minerals, including plagioclase.

As(III) Adsorption and Oxidation by Soil

The fractionation of added As(III) to three soils is shown in Fig. 1. The decrease in soluble As(III) was initially rapid for all soils, possibly reflecting strong initial adsorption on the available high-energy surface sites on metal oxides. The Fallbrook and Panoche soils displayed a greater amount of both adsorption and oxidation than the Indio soil. For all soils, total recoverable As decreased steadily for 48 h, probably due to slow intraparticle diffusion of both As(III) and As(V). Rapid adsorption was followed by oxidation of As(III) to As(V), which then partitioned between the solid and solution phases (Fig. 1). Soluble As(V) was detected immediately after As(III) contacted the soil, and both As(III) and As(V) were recovered in PO_4 extracts of the soil solids. The overall reaction behavior involved an initial, fast As(III) adsorption reaction followed by both oxidation to As(V), and an immobilization reaction where both As(III) and As(V) were incorporated into the solid phase. Arsenic(III) may be adsorbed and stabilized on certain mineral surface sites in soil, especially Fe oxides (Manning et al., 1998); however, the recovery of exchangeable As(III) in the 10 mM PO_4 extract decreased with time.

Based on the general behavior of As(III) (Fig. 1), a hypothetical reaction scheme to describe the dominant reaction pathways for As(III) in aerobic soils was postulated (Fig. 2). Soluble As(III) is rapidly adsorbed on mineral surfaces such as Fe oxides and phyllosilicate edge sites to form As(III) complexes, which are partially recoverable with PO_4 (denoted exchangeable [$\equiv\text{Me}-\text{As}(\text{III})$]). The scheme in Fig. 2 indicates that certain mineral surfaces, such as Mn oxides, cause heterogeneous oxidation of As(III) by formation of a precursor

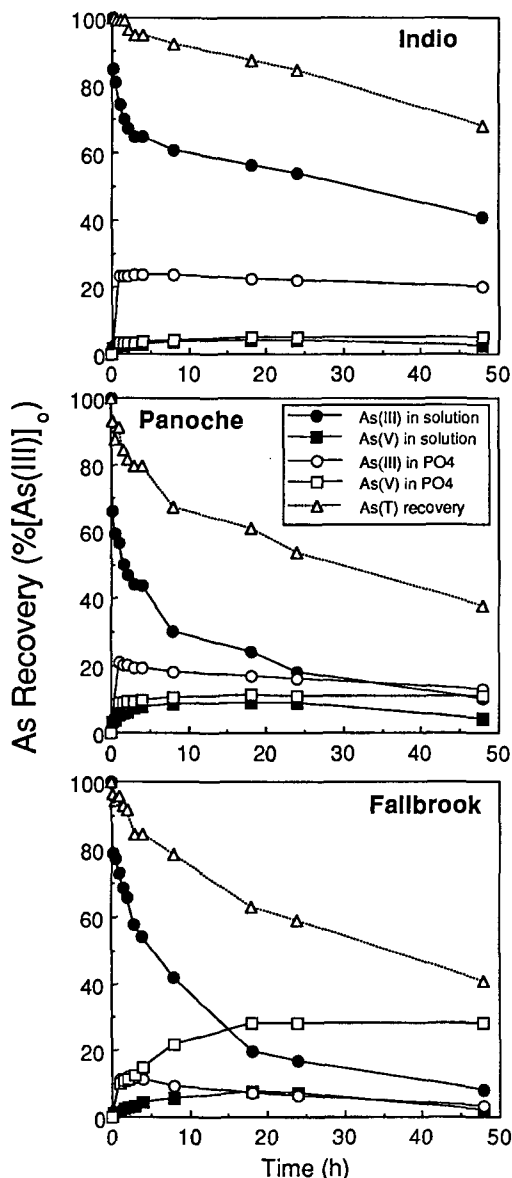


Fig. 1. Fractionation of As(III) and As(V) in As(III)-treated Indio, Panoche, and Fallbrook soils as a function of time. The pH values in the As(III) reaction solutions for the three soils were 6.5, 7.9, and 9.3 for Fallbrook, Panoche, and Indio soil, respectively.

complex (denoted $[=Mn-As(III)]$) followed by release of the As(V) reaction product into solution. This pathway has been recognized previously for the reaction of As(III) on synthetic Mn oxides (Scott and Morgan, 1995; Sun and Doner, 1998). Homogeneous As(III) oxidation was not observed in solutions that had not been in contact with soil, or in filtered soil suspension supernatants, and thus was not considered as an important reaction pathway for As(III). The long-term fate of As(III) added to soil involves adsorption, heterogeneous oxidation on certain mineral surfaces, and intraparticle diffusion. Ultimately, the formation of immobile As(III) and As(V) may involve reaction pathways that are unknown (designated as “?” in Fig. 2). It is important to note that the consecutive reaction model employed in this study uses apparent rate laws that are combinations of the

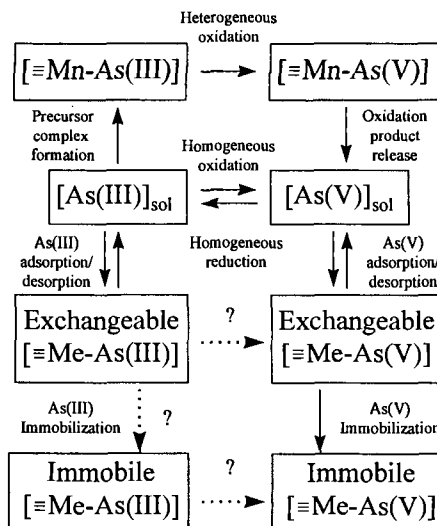


Fig. 2. Hypothetical reaction pathways for As(III) and As(V) in soil. In this figure, $=Mn$ denotes a manganese oxide surface complex, whereas $=Me$ denotes all other oxide mineral surfaces that bind As in soil.

elementary reaction steps indicated in Fig. 2. The reaction steps in Fig. 2 are consistent with, and reflected in, our experimental results but remain hypothetical because of the macroscopic nature of this study.

Effects of Soil Properties on As(III) Adsorption and Oxidation

The effect of pH on the reactions of As(III) with the Fallbrook soil was investigated in detail because this soil had the greatest As(III) oxidizing capacity. Increasing the Fallbrook soil suspension pH caused an increase in the initial As(III) adsorption rate, though the amount of soluble As(III) converged for the four treatments after 48 h (Fig. 3a). The more rapid adsorption of As(III) in the higher pH treatment was reflected in the increases in fitted rate constants to describe changes in $[As(III)]_{sol}$ as the suspension pH was increased from 5 to 8 (Table 2). Increasing pH caused an increase in the fitted rate constants to describe $[As(III)]_{Recov}$ for the early (fast) time period ($t < 2$ h), but the effects of pH on the rate constants to describe the slow rate of change in $[As(III)]_{Recov}$ (k_{slow}) were less obvious (Table 2). Increases in the recovery of As(III) in the PO_4 extract (Fig. 3b) corresponded with increases in adsorption. Combining the $[As(III)]_{sol}$ and $[As(III)]_{exch}$ fractions shows that total As(III) recovered ($[As(III)]_{sol} + [As(III)]_{exch}$) was only slightly effected by pH (Fig. 3c). At the suspension density and initial As(III) concentration used in this study, pH had the greatest effect on the short-term solid-water partitioning of As(III). Recent work (Raven et al., 1998; Manning et al., 1998; Manning and Goldberg, 1997b) has shown that Fe oxides, amorphous Al oxide, and aluminosilicate minerals have a maximum equilibrium affinity for As(III) near pH 9.2. This behavior is consistent with the increase in As(III) adsorption rate observed when pH was increased from 5.0 to 8.0 in As(III)-treated Fallbrook suspensions.

The level of soluble As(V) in As(III)-treated Fall-

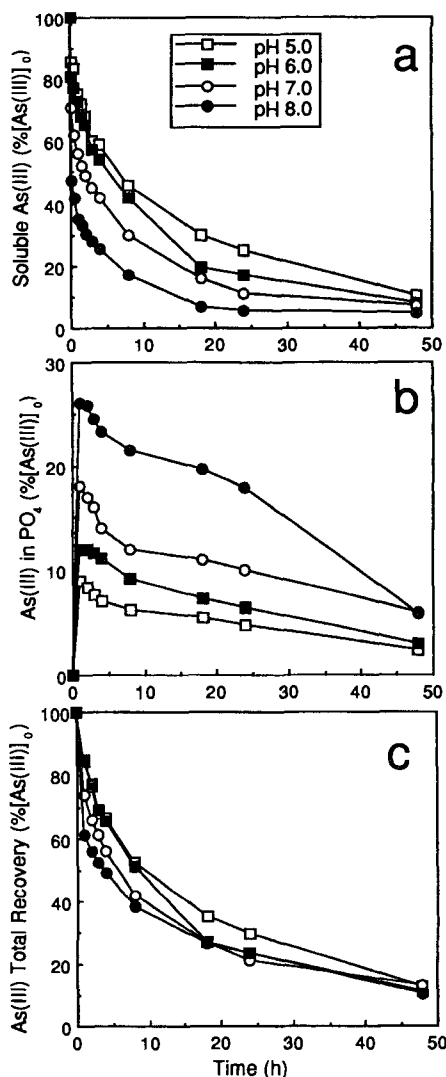


Fig. 3. (a) Effect of pH and time on soluble As(III), (b) PO_4 -exchangeable As(III), and (c) total recoverable As(III) in As(III)-treated Fallbrook soil.

brook reached a maximum at 18 h and then decreased with time. The greatest concentration of soluble As(V) was observed at the lowest pH (Fig. 4a), which suggested that a mineral surface reaction was participating in the oxidation of As(III) in soils. Previous investigation of the pH dependence of As(III) oxidation by δ - MnO_2 (Scott and Morgan, 1995) determined that the reaction rate increases with decreasing pH. However, in more

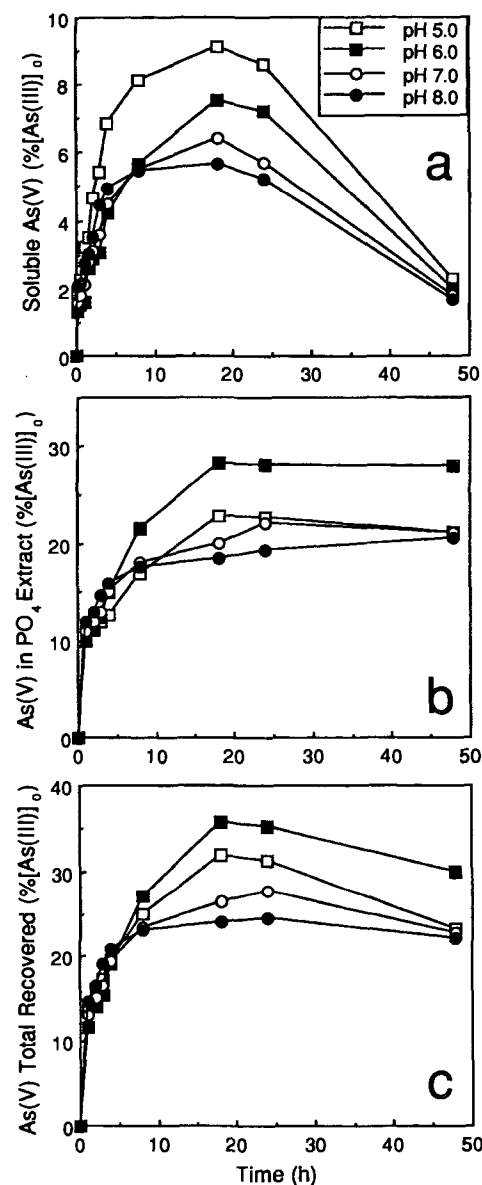


Fig. 4. (a) Effect of pH and time on soluble As(V), (b) exchangeable As(V), and (c) total recoverable As(V) in As(III)-treated Fallbrook soil.

complex systems such as soil, oxidation and adsorption are operating simultaneously. This probably explains the greater recovery of As(V) at pH 6.0 than pH 5.0 (Fig. 4b and 4c) because even though more As(V) is

Table 2. Empirical, fitted reaction rate constants for the reactions of As(III) with Indio, Panoche, and Fallbrook soils.

Soil	pH	Case 1†			Case 2‡		
		$k_{1\text{fast}}^\ddagger$	$k_{1\text{slow}}$	k_2	$k_{1\text{fast}}^\ddagger$	$k_{1\text{slow}}$	k_2
Indio	9.1	0.1780	0.0101	0.2210	0.0496	0.0082	0.0850
Panoche	8.3	0.3034	0.0327	0.2280	0.1948	0.0222	0.0791
Fallbrook	6.5	0.1709	0.0445	0.3900	0.1327	0.0412	0.0440
	5.0§	0.1710	0.0431	0.3170	0.1345	0.0368	0.0465
	6.0	0.1760	0.0614	1.023	0.1280	0.0412	0.0390
	7.0	0.2990	0.0669	1.126	0.2080	0.0342	0.0514
	8.0	0.4650	0.0831	1.325	0.2905	0.0349	0.0576

† See Theory section for rate equations used in the consecutive reaction model and explanation of Case 1 and Case 2.

‡ Fast reaction is $t < 2$ h; slow reaction is $t > 2$ h. Units of k are per hour. See Theory section for complete definitions of $k_{1\text{fast}}$, $k_{1\text{slow}}$, and k_2 .

§ Fallbrook pH adjusted to 5.0, 6.0, 7.0, and 8.0 with HCl-NaOH.

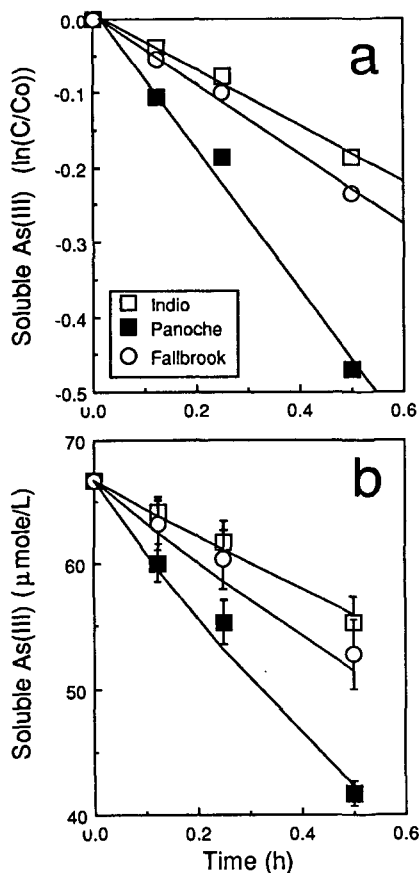


Fig. 5. Fitting a rate expression to soluble As(III) data evaluated for $t = 0$ to 0.5 h: (a) normalized soluble As(III) data in As(III)-treated Indio, Panoche, and Fallbrook soils with linear regression fits and (b) comparison of the experimental data (points) with the prediction using Eq. [18] (lines).

formed at lower pH, the As(V) species also is adsorbed more strongly at low pH and is more resistant to extraction by PO_4 . The effect of pH on As(III) oxidation in soil appears to be twofold. First, increasing pH results in increases in the As(III) adsorption rate on most reactive surfaces (Fe and Al oxides), which effectively decreases the amount of As(III) available for heterogeneous oxidation by surfaces that oxidize As(III), such as Mn oxides. Second, decreasing pH results in more favorable conditions for heterogeneous oxidation of As(III) by Mn oxides, which has been confirmed in pure systems (Scott and Morgan, 1995; Sun and Doner, 1998).

In addition to pH, soil properties that affect the rapid As(III) adsorption rate are those which reflect the availability and reactivity of mineral surfaces, such as clay percentage, SA, and Me_T . After an analysis of the effects of soil properties on the rapid adsorption reaction of As(III), it was determined that the differences in the rapid ($t = 0$ –2 h) As(III) adsorption behavior between the soils was best explained by the differences in the product $[\text{Me}_T \times \text{pH}]$ of the soils. An increase in Me_T is an indicator of increased reactive surface in the soil, and increasing soil pH increases the As(III) adsorption rate. The pH values in the As(III) reaction solutions for the Fallbrook, Panoche, and Indio soils were 6.5,

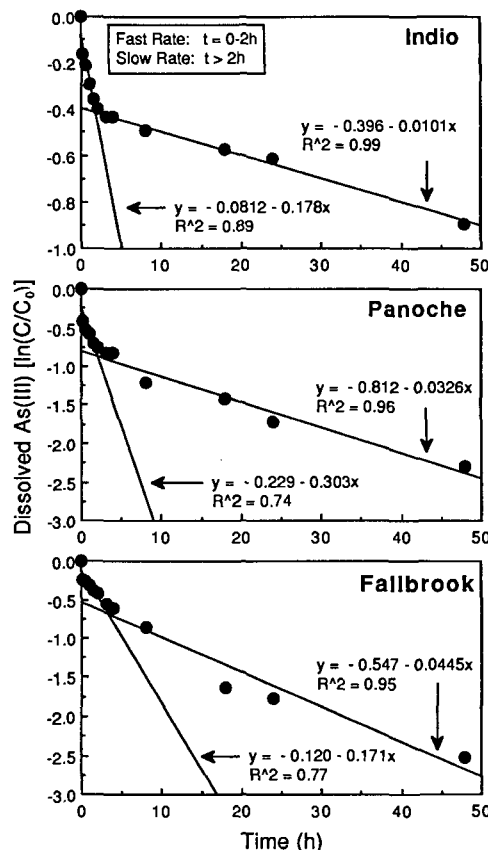


Fig. 6. Normalized soluble As(III) data in As(III)-treated Indio, Panoche, and Fallbrook soils with linear regression fits to the fast ($t < 2$ h) and slow ($t > 2$ h) time ranges.

7.9, and 9.3, respectively. The Aiken soil pH was 5.9 (discussed below).

Determination of the rapid adsorption reaction rate of As(III) on the Fallbrook, Panoche, and Indio soils for $t < 0.5$ h showed a roughly linear decrease in soluble As(III) in normalized data $[\ln(C/C_0)]$ for this short time (Fig. 5a). Three soil-specific rate constants ($k_{1\text{fast}}^{\text{soil}_i}$) were calculated using the three slopes derived from the experimental data in Fig. 5a. The ($k_{1\text{fast}}^{\text{soil}_i}$) values were then normalized to determine a constant for the three soils:

$$k_{1\text{fast}}^N = \frac{\sum_i^n \{k_{1\text{fast}_i}^{\text{soil}_i} [(\text{Me}_T)_i \text{pH}_i]^{-1}\}}{n} \quad [17]$$

After calculation of ($k_{1\text{fast}}^N$), a rate expression was developed for predicting the decrease in $[\text{As(III)}]_{\text{sol}}$ for an individual soil which is analogous to Eq. [16]:

$$[\text{As(III)}]_{\text{sol}}^{\text{soil}_i} = [\text{As(III)}]_0 \exp[-k_{1\text{fast}}^N (\text{Me}_T)_i \text{pH}_i t] \quad [18]$$

The results of inserting the values for Me_T and pH from Table 1 into Eq. [18] are shown as lines in Fig. 5b and good agreement between experimental data and the model was found for the rapid decrease in $[\text{As(III)}]_{\text{sol}}$ observed in the soils. Because SA and Me_T were correlated in the four soils (Table 1) it was not necessary to simultaneously include both of these properties in Eq. [18]. Though ($k_{1\text{fast}}^N$) may not be appropriate for all soils, it probably represents soils containing similar mineral phases as the soils from which the values were obtained.

Prediction of $[\text{As(III)}]_{\text{sol}}$ across longer time periods ($t = 0\text{--}48$ h) was achieved by deriving the rate constants directly from $[\text{As(III)}]_{\text{sol}}$ data (Fig. 6) followed by normalization of the rate constants with soil properties. The plots of $\ln(C/C_0)$ vs. t showed two time regions at $t < 2$ h and $t > 2$ h, which necessitated the designation of a fast rate ($k_{1\text{fast}}$, $t < 2$ h) and a slow rate ($k_{1\text{slow}}$, $t > 2$ h) for accurately describing the rate of removal of As(III) from solution. This two-rate behavior probably results from rapid initial adsorption of As(III) on high-energy surface sites, followed by slower processes that affect $[\text{As(III)}]_{\text{sol}}$, such as intraparticle diffusion into soil particles and oxidation on mineral surfaces.

After determination of ($k_{1\text{fast}}$) and ($k_{1\text{slow}}$) (Fig. 6), the ($k_{1\text{slow}}^N$) for each soil was used in an equation analogous to Eq. [11] and k_{2i} was optimized for describing $[\text{As(V)}]_{\text{sol}}$ and $[\text{As}]_{\text{immobile}}$. The values for k_{2i} were determined by minimizing the variance between measured and modeled values of $[\text{As(V)}]_{\text{sol}}$. The soil-specific rate constants were then normalized by soil properties as described in Eq. [14] to [16] using Me_T , Mn_{OX} , pH, and soil texture. The resulting constants for inclusion in the consecutive reaction model are defined in Table 3. The definitions in Table 3 indicate that the behavior of As(III) in an unknown soil would be predicted by knowing Me_T , pH, Mn_{OX} , soil texture, and $[\text{As(III)}]_0$. Though pH was successfully incorporated into the rate constants for describing $[\text{As(III)}]_{\text{sol}}$ in the 0- to 2-h time period [rapid As(III) adsorption], this was the only case where pH affected the apparent reaction rate. For longer time periods, the majority of the difference among $[\text{As(III)}]_{\text{sol}}$, $[\text{As(V)}]_{\text{sol}}$, and $[\text{As(III)}]_{\text{recov}}$ was accounted for by Me_T and Mn_{OX} alone (Table 3). The rate constants used to predict $[\text{As(V)}]_{\text{recov}}$ were normalized using Mn_{OX} and sand percentage because the Fallbrook soil, which had a combination of the highest Mn_{OX} (of the three soils) and a coarse texture (66% sand), yielded the most $[\text{As(V)}]_{\text{recov}}$.

Describing As(III) Reactions with the Consecutive Reaction Model

Using the rate constants described in Table 3, the consecutive reaction rate model was used to describe the fractionation of As(III) in soil suspensions over the entire measurement time period ($t = 0\text{--}48$ h). Soluble As(III) and As(V) were described using Case 1 (Eq. [3]), which includes the prediction of $[\text{As}]_{\text{immobile}}$. Comparing the soil property-normalized consecutive reaction rate model results with the soluble As(III) and As(V) experimental data for the Fallbrook, Panoche, and Indio soils (Fig. 7) indicates that the model gives a good description of the general trends of the $[\text{As(III)}]_{\text{sol}}$ and $[\text{As(V)}]_{\text{sol}}$ data. However, the $[\text{As}]_{\text{immobile}}$ fraction is somewhat overpredicted at $t > 18$ h in the Panoche and Fallbrook soils. Using recoverable As(III) and As(V) (Case 2, Eq. [4]) in the consecutive reaction rate model also resulted in an excellent description of the experimental results, with the exception of short-term $[\text{As}]_{\text{immobile}}$ data ($t < 24$ h), which were somewhat underpredicted (Fig. 8). Comparing model results suggests

Table 3. Definitions of soil property-normalized rate constants used in the consecutive reaction model to describe the reactions of As(III) with soil.

Model†	Time	Fraction	Rate constant definition
Case 1	<2 h	$[\text{As(III)}]_{\text{sol}}$	$k_{1\text{fast}} = 2.16 \times 10^{-4} \cdot \text{Me}_T \cdot \text{pH}^\ddagger$
	>2 h	$[\text{As(III)}]_{\text{sol}}$	$k_{1\text{slow}} = 1.09 \times 10^{-2} \cdot \text{Mn}_{\text{OX}}^\S$
	0–48 h	$[\text{As(V)}]_{\text{sol}}$, $[\text{As}]_{\text{immobile}}$	$k_{2i} = 0.147 + 0.0414 \cdot \text{Mn}_{\text{OX}}$
Case 2	<2 h	$[\text{As(III)}]_{\text{recov}}$	$k_{1\text{fast}} = 8.97 \times 10^{-4} \cdot \text{Me}_T$
	>2 h	$[\text{As(III)}]_{\text{recov}}$	$k_{1\text{slow}} = 8.86 \times 10^{-3} \cdot \text{Mn}_{\text{OX}}$
	0–48 h	$[\text{As(V)}]_{\text{recov}}$, $[\text{As}]_{\text{immobile}}$	$k_{2i} = 8.86 \times 10^{-3} \cdot \text{Mn}_{\text{OX}}$ $k_2 = 2.89 \cdot (\% \text{ Sand})^{-1}$

† See Theory section for rate equations used in the consecutive reaction model and definitions of Case 1 and Case 2.

‡ Me_T = total citrate-dithionite extractable metals ($\text{Al}_{\text{CD}} + \text{Fe}_{\text{CD}} + \text{Mn}_{\text{CD}}$, mmol kg^{-1}).

§ Mn_{OX} = ammonium oxalate-extractable manganese (mmol kg^{-1}).

that both modeling approaches (Case 1 and Case 2) can be used as indicators for predicting the formation of $[\text{As}]_{\text{immobile}}$.

The final step in the analysis of the consecutive reaction rate model involved describing the reaction of As(III) with an independent soil using the measured soil properties (Me_T , Mn_{OX} , pH, and soil texture) and the rate constants defined in Table 3. The Aiken soil sample, which was derived from volcanic parent materials, contained higher levels of extractable metals and had a lower pH than the other soils (Table 1). Although the Aiken soil contains high levels of extractable Mn,

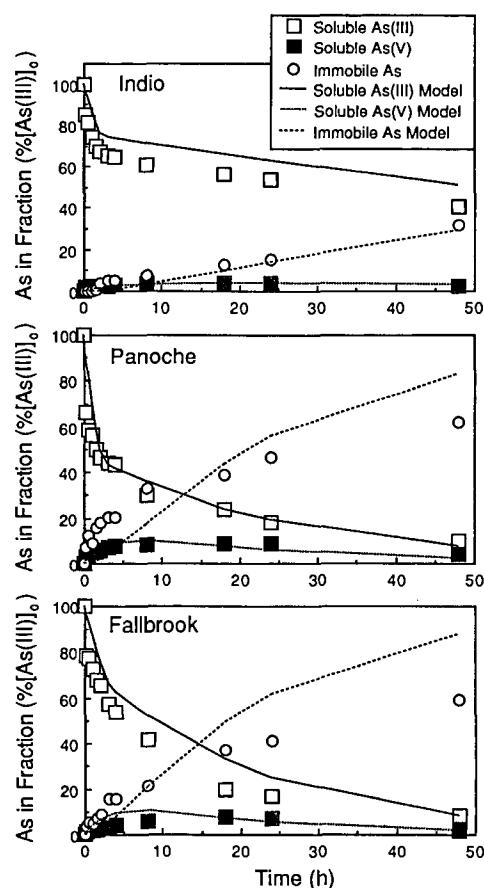


Fig. 7. Fit of the consecutive reaction rate model to soluble As(III) and As(V) in As(III)-treated Indio, Panoche, and Fallbrook soils.

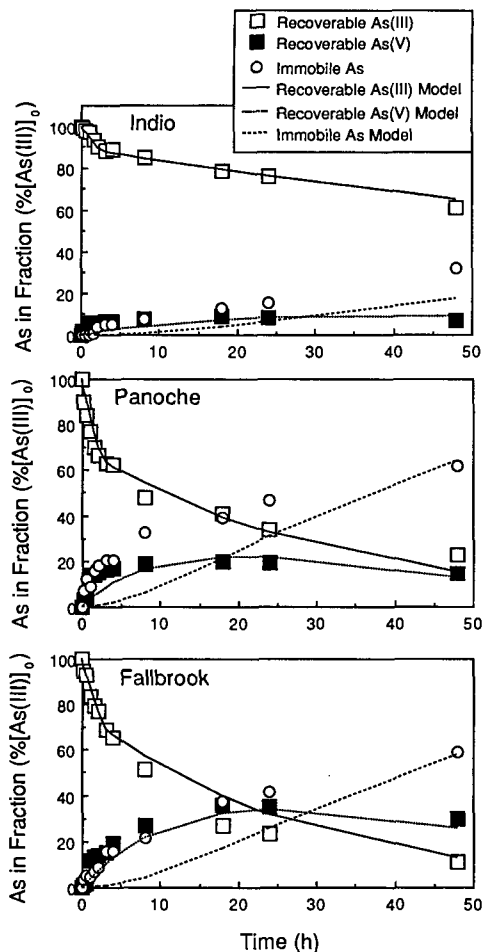


Fig. 8. Fit of the consecutive reaction rate model to recoverable As(III) and As(V) in As(III)-treated Indio, Panoche, and Fallbrook soils.

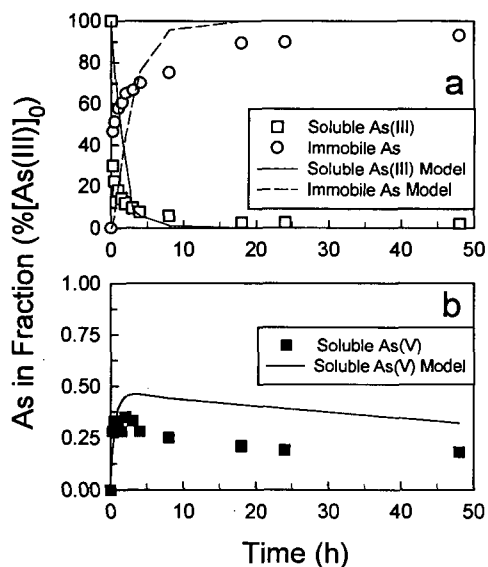


Fig. 9. Fit of the consecutive reaction rate model to (a) soluble As(III) and immobile As and (b) soluble As(V) in As(III)-treated Aiken soil.

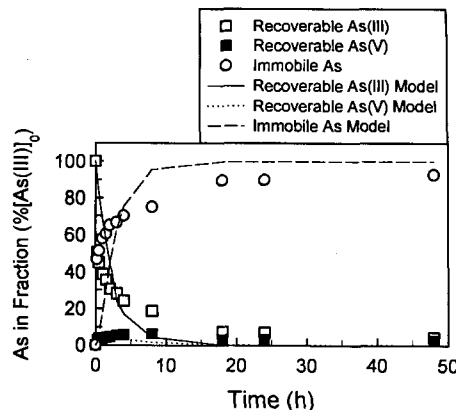


Fig. 10. Fit of the consecutive reaction rate model to recoverable As(III), recoverable As(V), immobile As in As(III)-treated Aiken soil.

the As(V) produced was resistant to recovery with 10 mM PO_4 because of the higher surface area and high levels of extractable metals (Me_T). Comparing the Aiken soil experimental data and the model results for $[\text{As(III)}]_{\text{sol}}$ and $[\text{As(V)}]_{\text{sol}}$ (Fig. 9a) shows clearly that the model accounts for the increase in the As(III) adsorption rate for this soil. The formation of the low level of soluble As(V) is also predicted by the model (Fig. 9b). Similarly, the model fit to the $[\text{As(III)}]_{\text{Recov}}$ and $[\text{As(V)}]_{\text{Recov}}$ data for the Aiken soil (Fig. 10) is reasonable considering that the Aiken soil properties are outside the range of soil property values for the Fallbrook, Panoche, and Indio soils, which were used to optimize the model.

CONCLUSIONS

The reactions of As(III) with the four soils included both adsorption and heterogeneous oxidation to As(V). A rapid As(III) adsorption reaction was followed by As(III) oxidation to As(V) and a partitioning of As(V) between the solution, exchangeable, and immobilized fractions of the soils. Soil properties important in determining the rate of As(III) adsorption in soil are those that affect the distribution and availability of reactive mineral surfaces, such as clay percentage, SA, pH, and levels of reactive metal oxides (Al, Fe, and Mn). Detailed experiments on the Fallbrook soil showed that pH had a pronounced effect on the initial, fast adsorption reaction of As(III) within this soil. However, among soils, other soil properties that reflect the amount of reactive surface will be more important than pH in explaining a soil's adsorption capacity.

Heterogeneous oxidation of As(III) will increase with increasing amounts of Mn oxide surfaces in the soil. However, due to the tendency of As(V) to form strong, inner-sphere complexes on metal oxide mineral surfaces, the recovery of As(V) will be more difficult in finer-textured soils due to their greater overall adsorption capacity. Though there was measurable heterogeneous As(III) oxidation in all four soils, the Fallbrook soil sample yielded the most recoverable As(V). We suspect that this was due to a combination of Fallbrook

soil properties (a critical amount of Mn oxide content and a coarse soil texture). The Aiken soil, which had elevated Mn compared with the other soils and was fine textured, had very low As(V) recovery. The long-term fate of As(III) in mineral soils under aerobic conditions involved oxidation to As(V) followed by the formation of unrecoverable or strongly adsorbed As(V). It is also possible that some unrecoverable (immobile) As(III) remained in the soil.

Developing a model to describe the kinetics of As(III) reactions in soils will be useful for predicting the fate and transport of As(III) and As(V) in column studies as well as the long-term disposition of As in the field. In addition, other elements such as Cr and Se, whose solubility and toxicity depend on redox state, will require a similar type of model development. The kinetics model used in this study (the consecutive reaction rate model) was developed for mineral soils and was used in combination with soil property measurements to describe both the adsorption and oxidation of As(III). Though model development will clearly be improved with the incorporation of more soil measurements, the model gave satisfactory descriptions of the behavior of both soluble and recoverable As(III) and As(V) in soil suspensions. Application of kinetic expressions to the reactions of As(III) with soil underscores the need for understanding the effects of soil physical and chemical properties on the adsorption and oxidation capacities of soils.

ACKNOWLEDGMENTS

This research was supported by the USDA National Research Initiative Competitive Grants Program (Project 9604171).

REFERENCES

- Elkhatib, E.A., O.L. Bennett, and R.J. Wright. 1984. Arsenite sorption and desorption in soils. *Soil Sci. Soc. Am. J.* 48:1025-1030.
- Fendorf, S., M.J. Eick, P. Grossl, and D.L. Sparks. 1997. Arsenate and chromate retention mechanisms on goethite. *Environ. Sci. Technol.* 31:315-320.
- Fordham, A.W., and K. Norrish. 1979. Arsenate-73 uptake by components of several acid soils and its implications for phosphate retention. *Aust. J. Soil Res.* 17:307-316.
- Fordham, A.W., and K. Norrish. 1974. Direct measurement of the composition of soil components which retain added arsenate. *Aust. J. Soil Res.* 12:165-172.
- Gee, G.W., and J.W. Bauder. 1986. Particle-size analysis. p. 383-411. *In* A. Klute (ed.) *Methods of soil analysis*. Part 1. 2nd ed. Agron. Monogr. 9. ASA and SSSA, Madison, WI.
- Holmgren, G.G.S. 1967. A rapid citrate-dithionite extractable iron procedure. *Soil Sci. Soc. Am. Proc.* 31:210-211.
- Jacobs, L.W., J.K. Syers, and D.R. Keeney. 1970. Arsenic sorption by soils. *Soil Sci. Soc. Am. Proc.* 34:750-754.
- Knowles, F.C., and A.A. Benson. 1983. The biochemistry of arsenic. *Trends Biochem. Sci.* 8:178-180.
- Korte, N.E., and Q. Fernando. 1991. A review of arsenic(III) in groundwater. *Crit. Rev. Environ. Control* 21:1-39.
- Laidler, K.J., and J.H. Meiser. 1982. *Physical chemistry*. Benjamin Cummings, Menlo Park, CA.
- Livesey, N.T., and P.M. Huang. 1981. Adsorption of arsenate by soils and its relation to selected chemical properties and anions. *Soil. Sci.* 131:88-94.
- Loeppert, R.L., and W.P. Inskeep. 1996. Iron. p. 639-664. *In* D.L. Sparks et al. (ed.) *Methods of soil analysis*. Part 3. SSSA Book Ser. 5. SSSA, Madison, WI.
- Manning, B.A., and S. Goldberg. 1997a. Arsenic(III) and arsenic(V) adsorption on three California soils. *Soil Sci.* 162:886-895.
- Manning, B.A., and S. Goldberg. 1997b. Adsorption and stability of arsenic(III) at the clay mineral-water interface. *Environ. Sci. Technol.* 31:2005-2011.
- Manning, B.A., and D.A. Martens. 1997. Speciation of arsenic(III) and arsenic(V) in sediment extracts by high performance liquid chromatography-hydride generation atomic absorption spectrophotometry. *Environ. Sci. Technol.* 31:171-177.
- Manning, B.A., S.E. Fendorf, and S. Goldberg. 1998. Surface structures and stability of arsenic(III) on goethite: Spectroscopic evidence for inner-sphere complexes. *Environ. Sci. Technol.* 32:2383-2388.
- McGeehan, S.L., and D.V. Naylor. 1994. Sorption and redox transformation of arsenite and arsenate in two flooded soils. *Soil Sci. Soc. Am. J.* 58:337-342.
- Oscarson, D.W., P.M. Huang, and W.K. Liaw. 1980. The oxidation of arsenic by aquatic sediments. *J. Environ. Qual.* 9:700-703.
- Oscarson, D.W., P.M. Huang, and W.K. Liaw. 1981. Role of manganese in the oxidation of arsenite by freshwater lake sediments. *Clays Clay Miner.* 29:219-225.
- Oscarson, D.W., P.M. Huang, W.K. Liaw, and U.T. Hammer. 1983. Kinetics of oxidation of arsenite by various manganese oxides. *Soil Sci. Soc. Am. J.* 47:644-648.
- Pierce, M.L., and C.B. Moore. 1982. Adsorption of arsenite and arsenate on amorphous iron oxyhydroxide. *Water Res.* 16:1247-1253.
- Raven, K.P., A. Jain, and R.H. Loeppert. 1998. Arsenite and arsenate adsorption on ferrihydrite: Kinetics, equilibrium, and adsorption envelopes. *Environ. Sci. Technol.* 32:344-349.
- Scott, M.J., and J.J. Morgan. 1995. Reactions at oxide surfaces. 1. Oxidation of As(III) by synthetic birnessite. *Environ. Sci. Technol.* 29:1898-1905.
- Skopp, J. 1986. Analysis of time-dependent chemical processes in soils. *J. Environ. Qual.* 15:205-213.
- Sparks, D.L. 1989. *Kinetics of soil chemical processes*. Academic Press, San Diego, CA.
- Steel, R.G.D., and J.H. Torrie. 1980. *Principles and procedures of statistics: A biometrical approach*. 2nd ed. McGraw-Hill, New York.
- Sun, X., and H.E. Doner. 1996. An investigation of arsenate and arsenite bonding structures on goethite by FTIR. *Soil Sci.* 161:865-872.
- Sun, X., and H.E. Doner. 1998. Adsorption and oxidation of arsenite on goethite. *Soil Sci.* 163:278-287.
- Waychunas, G.A., B.A. Rea, C.C. Fuller, and J.A. Davis. 1993. Surface chemistry of ferrihydrite: Part 1. EXAFS studies of the geometry of coprecipitated and adsorbed arsenate. *Geochim. Cosmochim. Acta* 57:2251-2269.